GJR Publication
OPEN ACCESS

Global Journal of Research in Engineering & Computer Sciences
ISSN: 2583-2727 (Online)
Volume 05| Issue 03 | May-June | 2025
Journal homepage: https://gjrpublication.com/gjrecs/

Research Article

A Generalized Hybrid Nanofluid Model Transports with Magnetic, Suction, Velocity Slip, And Varying Viscosity and Thermal Conductivity

[1] M. S. Dada and [2] F. J. Fawehinmi*

[1] Department of Mathematics, Faculty of Physical Sciences, University of Ilorin, Nigeria
[2] Faculty of Science Education, Adeyemi Federal University of Education, Ondo, Nigeria

DOI: 10.5281/zenodo.15731771 **Submission Date: 20 May 2025 | Published Date: 24 June 2025**

Corresponding author: F. J. Fawehinmi
Faculty of Science Education, Adeyemi Federal University of Education, Ondo, Nigeria

Abstract

A mathematical model was developed for a generalised copper/alumina-water hybrid nanofluid, which is affected by magnetic fields, suction, velocity slip, and variations in viscosity and thermal conductivity along a convectively heated stretched sheet. The governing equations were converted into nonlinear ordinary differential equations using a similarity transformation. By employing the BVPh function in MATHEMATICA, our results align with those obtained from bvp4c and ode45, thereby ensuring convergence through a control parameter within the homotopy analysis framework. The results indicated that increasing the variable viscosity parameter, unsteady parameter, and nanofluid volume fractions led to an increase in both the skin friction coefficient and local Nusselt number. The velocity profile increased with the stretching parameter from 0 to 1, whereas the magnetic field parameter and variable thermal conductivity had a smaller effect on the local Nusselt number and skin friction coefficient.

Keywords: *hybrid nanofluid, similarity transformation, BVPh, convergencecontrol parameter, homotopy.*

1. Introduction

The capacity for heat transfer in standard heat transfer fluids (HTFs) as water and oil is limited. To address these limitations, a new category of HTFs called nanofluids was developed. Hybrid nanofluid (HNF) emerged from advancements in heat transfer technology, offering high efficiency in applications and lowering production costs. [38, 33, 28, 9]. The performance and efficiency of the heat transfer can influence the boundary conditions and thermophysical properties of the working fluid, such as its density, viscosity, specific heat, and thermal conductivity. [42, 14, 7, 1, 30, 27, 5].

Nanofluids are considered the future of heat transfer fluids, consisting of two-phase combinations such as solid-liquid, solid-gas, or solid-plasma [17, 3]. These are colloidal suspensions in which nanoparticles or nanoscale particles are dispersed in the base fluids, allowing them to conduct heat more effectively than the base fluids alone [39, 29, 31]. The concept of nanofluids was first proposed by Choi and Eastman in 1995 [11]. Owing to their distinctive properties, nanofluids are essential in various fields including microelectronics, pharmaceutical manufacturing, hybrid engines, household refrigerators, automotive industries, and mechanical engineering [34, 19, 13]. These particles are combined with a variety of common liquids including water, engine oil, alcohol, and glycerol. The particles consist of metallic materials, such as oxide particles, carbon nanotubes, graphene nanoflakes, carbides, nitrites, borides, carbon nanofibres, exfoliated graphite, nanodiamonds, nanocellulose, nanocrystals, and detonation nanodiamond-multiwalled carbon nanotubes (DND-CNT) [26, 25, 43]. In liquid environments, nanoparticles can interact with fluid particles, thereby enhancing their surface area and thermal efficiency. This interaction is crucial for applications in solar energy, biomedical treatment, and industrial processes [32, 44, 21].

By diluting compound nanopowders or various types of nanomolecules in a solution, a hybrid nanofluid containing multiple nanomaterials can be created [23]. These fluids are formulated by combining different nanoparticles within the

same base fluid to enhance their thermophysical, optical, rheological, and morphological properties. Because of their numerous advantages over single nanofluids, such as a wider absorption range, decreased extinction, superior thermal conductivity, lower pressure drop, and minimised frictional losses and pumping, HNFs are anticipated to replace simple nanofluids [26, 8, 18]. With a higher heat transfer coefficient than that of standard nanofluids, HNFs have become a focal point for many researchers exploring new study areas [35, 12]. Hybrid nanofluids are used in engine systems, machine cutting, automotive cooling, photovoltaic thermal (PV/T) management, machine collectors, and thermal management of electronic components [20, 16, 45].

Researchers have explored the influence of changes in viscosity and thermal conductivity on fluids. Examples of these studies can be found in [4, 24]. Ali et al. (2017) [4] investigated a thin fluid layer with varying fluid properties across a stretching sheet, considering the effect of thermophoresis. The governing equations of the model were transformed into nonlinear coupled differential equations by using suitable similarity variables. These equations are then solved using the second approach of the Optimal Homotopy Asymptotic Method (OHAM-2). In addition, further research has been conducted [10, 48] on the effect of nanofluid parameters on the velocity and temperature fields. In their study, the residual error and results from the Homotopy Asymptotic Method (HAM) were quantitatively analysed.

A study comparing magnetohydrodynamic (MHD) flow near a stagnation point in hybrid nanofluids and regular nanofluids has been carried out [36, 37, 6, 22]. The findings indicated that the hybrid nanofluids were more effective as heaters than the nanofluids when the magnetic parameter was increased. However, owing to the increasing Eckert number, stretching, and velocity slip parameters, hybrid nanofluids also outperformed nanofluids as coolers. Furthermore, three stability zones were identified after analysing the stability of the unique/dual solution. In their 2020 research, Hayat *et al.,* [15] explored the impact of thermal radiation on the three-dimensional flow of nanofluids through carbon nanotubes. Their study included both single-wall and multi-wall carbon nanotubes (SW/MW-CNTs), and they utilised Optimal Homotopy Analysis methods to develop solutions.

A multitude of researchers have explored the concept of nanoscience and nanofluids, particularly in relation to traditional heat transfer challenges, aiming to improve the heat-transfer characteristics of various fluids [41]. Their work involved modelling factors such as thermal conductivity, variable viscosity, magnetic fields, and radioactive heat variations on flat, porous, and stretched surfaces. Usman et al. (2018) [40] studied the $Cu - Al_2O_3$/Water hybrid nanofluid on a permeable surface, taking into account both variable thermal conductivity and nonlinear radiation. Their study also focused on the time-dependent thermal conductivity. A systematic investigation of CO_2-silica (hydrophilic or hydrophobic) nanofluids considered the effects of pressure, temperature, salinity, and nanoparticle concentration [2] to assess the impact of nanofluid flooding on CO_2 geo-storage. Historically, many researchers examining hybrid nanofluids have not considered the effects of magnetism, suction, velocity slip, viscosity, and thermal conductivity simultaneously. In addition, they modelled the viscosity and thermal conductivity as temperature dependent. Consequently, this study aimed to expand the research field by exploring the influence of magnetic fields, suction, velocity slip, temperature-dependent viscosity, and thermal conductivity. Thus, a novel mathematical model for hybrid nanofluids is introduced. This work also seeks to address a gap in the literature by incorporating additional factors, such as heat generation, especially in the context of stagnation-point hybrid nanofluid flow. To address this issue, the BVPh2.0 method from the MATHEMATICA package was employed. A comparative analysis showed a strong correlation between the current findings and previous studies, thus forming the second objective of the study. The results are presented in figures and tables. Overall, given the importance of stagnant flows in numerous industrial applications, it is believed that a comprehensive analysis of these flows should be enhanced alongside the application of mathematical expertise. These findings are expected to assist other researchers and experts in expanding their understanding of heat transfer.

2. Model Formulation

We examine the problem of a two-dimensional, unsteady, laminar, and incompressible boundary layer involving hybrid nanofluid stagnation point flow over a mixed convective heated sheet that can stretch or shrink. This sheet moves with variations in viscosity and thermal conductivity, influenced by magnetic fields, suction, and velocity slip conditions, as shown in Figure 1. The Cartesian coordinate system (x, y) is assumed such that the x-axis runs along the surface, whereas the y-axis is perpendicular to it. The velocity components u and v along the x-and y-axes, respectively, depend on both x and y. At the initial moment, $t = 0$, the reference

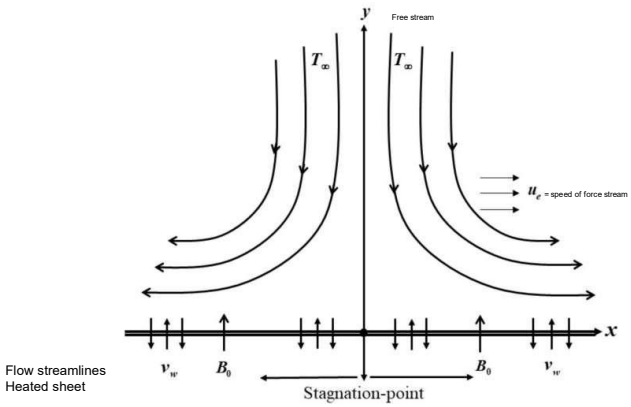

Figure 1: The model diagram

temperature is denoted by T_0, whereas the ambient temperature T_∞ is also referred to as the baseline or environmental air temperature at the base of the sheet, which is heated by convective heat, ensuring $0 \leq T_0 \leq T_\infty$. The temperatures at the base of the sheet, which vary with time and space owing to convective heating, are described by [46]: $T_w(x,t) = T_\infty + T_0 \frac{ax^2}{2\nu}(1-ct)^{-3/2}$, where $a > 0$ denotes the intensity of the stagnant flow, v is the velocity component along the y-axis, and c represents the unsteadiness factor, which indicates a temporal issue. The velocity for stretching or shrinking, $u_w(x,t)$, is expressed by [46] as $u_w(x,t) = \frac{bx}{1-ct}$, where b denotes the constant for the stretchable ($b > 0$) and shrinkable ($b < 0$) scenarios, and c signifies the time-related issue. The velocity of the force stream $u_e(x,t)$ is defined by [47] as $u_e(x,t) = \frac{ax}{1-ct}$. The dynamic viscosity of the hybrid nanofluid, which depends on temperature, was modified as follows:

$$\mu_{hnf}(T) = \mu_{hnf}(1 - \Lambda\theta(\eta)). \tag{1}$$

In this context, μ_{hnf} represents the viscosity of the hybrid nanofluid at the initial or ambient temperature T_0, Λ denotes the parameter for variable viscosity, and θ is the temperature expressed in a dimensionless form.

The thermal conductivity of the hybrid nanofluid, which varies with time, is described by:

$$K_{hnf}(T) = K_{hnf}(1 + \epsilon\theta(\eta)). \tag{2}$$

In this scenario, ϵ signifies the variable thermal conductivity parameter, θ is defined as previously mentioned, and K_{hnf} represents the thermal conductivity of the hybrid nanofluids. At the starting point $t = 0$, both the surface temperature $T_w(x,t)$ and the temperature of the hybrid nanofluid T are assumed to match the ambient temperature T_∞, which is the temperature of the surrounding fluid or the free stream. Furthermore, it is assumed that the hybrid nanofluid flows under the influence of the applied magnetic and electric fields, characterised by their respective magnetic, electric, and heat-generating properties $B_0(t)$, $E_0(t)$, and $Q_0(t)$. The governing equations for this analysis, which include the continuity, momentum, and energy equations for the hybrid nanofluid, are outlined below, considering the previously mentioned assumptions and conditions.

$$\frac{\partial u}{\partial x} + \frac{\partial v}{\partial y} = 0, \tag{3}$$

$$\frac{\partial u}{\partial t} + u\frac{\partial u}{\partial x} + v\frac{\partial u}{\partial y} = \frac{\partial u_e}{\partial t} + u_e\frac{\partial u_e}{\partial x} + \frac{1}{\rho_{hnf}}\frac{\partial}{\partial_y}(\mu_{hnf}(1 - \Lambda\theta(\eta))\frac{\partial u}{\partial y}) + \frac{\sigma_{hnf}}{\rho_{hnf}}(E_0(x,t)B_0(t) - B_0^2(t)(u - u_e)), \tag{4}$$

$$\frac{\partial T}{\partial t}+u\frac{\partial T}{\partial x}+v\frac{\partial T}{\partial y}=\frac{1}{(\rho C_p)_{hnf}}\frac{\partial}{\partial y}(K_{hnf}(1+\epsilon\theta(\eta))\frac{\partial T}{\partial y})+\frac{\mu_{hnf}(1-\Lambda\theta(\eta))}{(\rho C_p)_{hnf}}(\frac{\partial u}{\partial y})^2$$
$$+\frac{\sigma_{hnf}}{(\rho C_p)_{hnf}}(B_0(t)(u-u_e)-E_0(x,t)B_0(t))^2+\frac{Q_0}{(\rho C_p)_{hnf}}(T-T_\infty), \quad (5)$$

Subjected to the following boundary conditions:

$$u=u_w(x,t)+\nu H_1\frac{\partial u}{\partial y},\ -K_{hnf}\frac{\partial T}{\partial y}=h_f(T_w-T),\ \text{for } y=0; \quad (6)$$

and $v=0,\ T=T_w,$ for $y\to\infty;\ u\to u_e(x,t),\ T\to T_\infty,$

The variables u and v denote the velocity components in the x- and y-directions, respectively. Term u_e represents the speed of the force stream. The density of the hybrid nanofluid is denoted by ρ_{hnf} and its electrical conductivity is denoted by σ_{hnf}. The temperature of the hybrid nanofluid is denoted by T, where T_∞ represents the ambient temperature. The heat capacity of the hybrid nanofluid was expressed as (ρC_{phnf}). The expressions $\mu_{hnf}(T)$ and $K_{hnf}(T)$ refer to the dynamic viscosity and thermal conductivity, respectively, both of which vary with temperature. Parameters $B_0(t)$, $E_0(x,t)$, and $Q_0(t)$ are associated with the magnetic field, electric field, and heat generation characteristics, respectively, where t represents the time variable. By applying the following similarity variables,

$$\Psi=(\frac{av}{1-ct})^{1/2}xf(\eta),\ \theta(\eta)=\frac{T-T_\infty}{T_w-T_\infty},\ \eta=(\frac{a}{\nu(1-ct)})^{1/2}y, \quad (7)$$

where $\Psi=\Psi(x,t)$ is the physical stream function satisfying and we obtain the simplified boundary value problem equations (11-13):

$$(1+\Lambda\theta)f'''-\Lambda f''\theta'+(1+\Lambda\theta)^2[A_1(ff''-f'^2-\beta(f'+\frac{\eta}{2}f''))-A_2Mf'+\sigma_2]=0, \quad (8)$$

$$A_3PrE_cf''^2+(1+\Lambda\theta)[(1+\epsilon\theta)\theta''+\epsilon\theta'^2-Pr(A_4(2f'\theta-f\theta'+\frac{\beta}{2}(\eta\theta'+3\theta))$$
$$-A_5ME_c(f'^2-2Ef')^2-A_6Q\theta-\sigma_1)]=0, \quad (9)$$

Subjected to the boundary conditions

$$f(0)=0,\ f'(0)=\alpha+\gamma f''(0),\ -\frac{k_{hnf}}{k_f}\theta'(0)=Bi[1-\theta(0)],$$

$$f'(\eta)\to 1,\ \vartheta(\eta)\to 0,\ \text{as}\ \eta\to\infty, \quad (10)$$

where the non-dimensional variables and ratios are given respectively as:

$$\alpha=\frac{b}{a},\ \beta=\frac{c}{a},\ \gamma=H(a\nu)^{1/2},\ \nu=\frac{\mu}{\rho},\ E=\frac{E_0}{B_0\frac{ax}{1-ct}},\ M=\frac{\sigma_f B_0^2(t)(1-ct)}{a\rho_f},$$
$$E_c=\frac{u_e^2}{C_p(T_w-T_\infty)},\ Q=Q_0\frac{(1-ct)}{a},\ \text{and}\ P_r=\frac{\mu C_p}{K}, \quad (11)$$

$$A_1=\frac{\rho_{hnf}/\rho_f}{\mu_{hnf}/\mu_f},\ A_2=\frac{\sigma_{hnf}/\sigma_f}{\mu_{hnf}/\mu_f},\ A_3=\frac{\mu_{hnf}/\mu_f}{k_{hnf}/k_f},\ A_4=\frac{(\rho C_p)_{hnf}/(\rho C_p)_f}{k_{hnf}/k_f},$$
$$A_5=\frac{1/(\rho C_p)_f}{k_{hnf}/k_f}\qquad A_6=\frac{\sigma_{hnf}/\sigma_f}{k_{hnf}/k_f} \quad (12)$$

and

In this case, the stretching/shrinking parameter is denoted by α; the unsteadiness parameter is measured by β; the kinematic viscosity is denoted by ν; the velocity slip parameter is denoted by γ; the electric, magnetic, and heat

generation parameters are denoted by E, M, and Q, respectively; the Eckert and Prandtl numbers are denoted by E_c and Pr; and the magnetic and electric fields and heat generation characteristics are denoted by B_0, E_0, and Q_0. ...

3. Formulation of the Initial Guesses

The initial approximations $f_0(\eta)$ and $\theta_0(\eta)$ are derived by taking into account the boundary conditions specified in equation (22) and are selected as follows:

$$\theta 0(\eta) = b0 + b1e{-}\eta. \tag{13}$$

The above gives respectively

$$f_0(\eta) = \eta + c_0 + c_1 e^{-\eta},$$

$$f_0(\eta) = \eta + \frac{\alpha - 1}{\gamma + 1}(1 - e^{-\eta}), \tag{14}$$

$$\theta_0(\eta) = \left(\frac{Bi}{\frac{k_{hnf}}{k_f} + Bi}\right)e^{-\eta}$$

0.1 The physical properties of the hybrid nanofluid

The thermophysical properties of the hybrid nanofluid alumina-copper/water are presented in Table 1-2.

Table 1: The thermophysical properties of hybrid nanofluid: copper-alumina/water

Properties	k(W/mK)	$\rho(kg/m^3)$	C_p(J/kgK)	$\beta\times10^{-5}$(mK)
Cu	400	8933	385	1.67
Al2O3	40	3970	765	0.85
H_2O	0.613	997.1	4170	21

0.2 The Skin Friction Coefficient (C_f) and the Local Nusselt Number (Nu_x)

Two significant quantities that have drawn attention in technology and engineering are the skin friction coefficient (C_f) and local Nusselt number (Nu_x). By definition,

$$C_f = \frac{\tau_w}{\rho_f {u_e}^2}, \; Nu_x = \frac{x q_w}{K_f(T_w - T_\infty)} \tag{15}$$

Table 2: Correlations of the thermophysical properties

Properties	Hybrid nanofluid
Density	$\rho hnf = \phi s1\rho 1 + \phi s2\rho s2 + (1 - \phi hnf)\rho f$
Thermal capacity	(
Dynamic viscosity	$\rho C_p)_{hnf} = (\rho C_p)_{s1}\phi_1 + (\rho C_p)_{s2}\phi_2 + (\rho C_p)_f(1 - \phi_{hnf})$
Thermal conductivity	$\mu_{hnf} = \frac{\mu_f}{(1-\phi_{hnf})^{2.5}}$
Electric conductivity	$\frac{k_{hnf}}{k_f} = \left[\frac{\left(\frac{k_{s1}\phi_{s1}+k_{s2}\phi_{s2}}{\phi_{hnf}}\right)+2k_f+2(k_{s1}\phi_{s1}+k_{s2}\phi_{s2})-2\phi_{hnf}k_f}{\left(\frac{k_{s1}\phi_{s1}+k_{s2}\phi_{s2}}{\phi_{hnf}}\right)+2k_f-(k_{s1}\phi_{s1}+k_{s2}\phi_{s2})+\phi_{hnf}k_f}\right]$
Thermal expansion	$\frac{\sigma_{hnf}}{\sigma_f} = \left[\frac{\left(\frac{\sigma_{s1}\phi_{s1}+\sigma_{s2}\phi_{s2}}{\phi_{hnf}}\right)+2\sigma_f+2(\sigma_{s1}\phi_{s1}+\sigma_{s2}\phi_{s2})-2\phi_{hnf}\sigma_f}{\left(\frac{\sigma_{s1}\phi_{s1}+\sigma_{s2}\phi_{s2}}{\phi_{hnf}}\right)+2\sigma_f-(\sigma_{s1}\phi_{s1}+\sigma_{s2}\phi_{s2})+\phi_{hnf}\sigma_f}\right]$
	$\rho\beta)_{hnf} = \phi_{s1}\rho_{s1}\beta_{s1} + \phi_{s2}\rho_{s2}\beta_{s2} + (1 - \phi_{hnf})(\rho\beta)_f$ (

where x represents the horizontal direction (x-axis), τ_w is the shear stress along the x-direction, and q_w denotes the surface heat flux.

The shear stress (τ_w) and surface heat flux (q_w) are defined as

$$\tau_w = \mu_{hnf}(T)\frac{\partial u}{\partial y}|_{y=0} \text{ and}$$

$$q_w = -K_{hnf}(T)\frac{\partial T}{\partial y}|_{y=0} \tag{16}$$

By inserting equations (4), (5), (10), and (11) into equation (24) and then incorporating these into equation (23), we derive the following formulas for the Skin Friction Coefficient (C_f) and Local Nusselt Number (Nu_x), respectively:

$$\sqrt{Re_x}C_f = \frac{\mu_0/(1+\Lambda)}{\mu_f}f'' \tag{17}$$

$$\frac{1}{\sqrt{Re_x}}Nu_x = -\frac{K_0(1+\epsilon)}{K_f}\theta' \tag{18}$$

where $Re_x = \sqrt{\frac{a\rho_f x^2}{\mu_f(1-ct)}}$ is the local Reynolds number in the x-direction.

4. INTERPRETATION OF RESULT

Simplified coupled differential equations (11) and (12), along with boundary conditions (13), constitute a complex nonlinear boundary value problem. To address these nonlinear systems of third-order coupled boundary value problems, the Optimal Homotopy Asymptotic Method (OHAM) was utilised. Zhao's Mathematica package (Zhao, *et al.*, 2014) provides numerical solutions for these nonlinear differential equations that closely align with both exact solutions and other numerical solutions. Notably, this approach eliminates the need for discretisation, linearisation, or small perturbations, thereby reducing the computational time and effort. The solutions are presented and compared to the existing results when $\alpha = \beta = \gamma =$ E = M = E_c = Q = E_0 = Q_0 = 0, Bi = 0.1, $\epsilon = \Lambda = 0.5$, and Pr = 6.2. The results are consistent with the existing findings using other numerical methods, as shown in Table 3.

0.3 Interpretation of result

In this section, we present the results and discuss how variations in the parameters of the controlling hybrid nanofluid influence the velocity and temperature profiles as well as the skin function, Nusselt number, and Reynolds number. These findings are illustrated in the graphs below. Figure 2 depicts the velocity profile $f'(\eta)$ and temperature profile $\theta(\eta)$ under the conditions $\alpha = \beta$ $= \gamma =$ E = M = E_c = Q = E_0 = Q_0 = 0, Bi = 0.1, $\epsilon = \Lambda = 0.5$, and Pr = 6.2.

Table 3: Velocity and temperature components at convergence-control parameters $c_1 = -1.76377$, $c_2 = -0.524517$

λ	Present work ($f''(\eta)$)	Zainal *et al.*, 2021	Bachok *et al.*, 2010.	$\theta'(\eta)$	Error (f)	Error (θ)
0.0	1.232249	1.23259	1.23259	-0.094923	3.77454×10^{-6}	2.61958×10^{-6}
0.1	1.146682	1.14656	1.14656	-0.095539	4.46123×10^{-6}	2.90939×10^{-6}
0.2	1.051411	1.05113	1.05113	-0.095989	4.04950×10^{-6}	3.40386×10^{-6}
0.5	0.713504	0.71329	0.71329	-0.096835	1.48826×10^{-6}	4.62406×10^{-6}
2.0	-1.888444	-1.88731	-1.88731	-0.098128	1.82440×10^{-5}	1.24181×10^{-4}

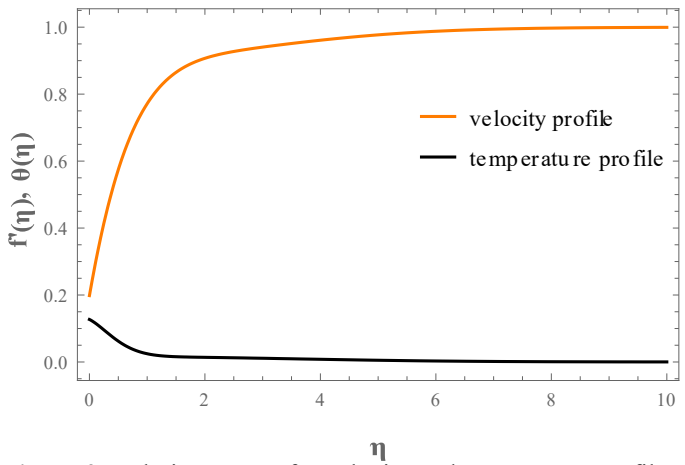

Figure 2: Solution curves for velocity and temperature profiles

Figure 2 illustrates a function for the velocity profile that increases positively, and a function for the temperature profile that decreases positively with respect to the independent variable η. It should also be noted that the velocity profile

increases when the flow is near the boundary, whereas the temperature profile decreases when it is very close to the boundary. Figure 3 shows

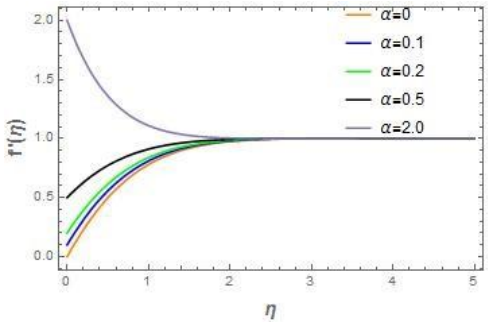

(a) Velocity profile for variants stretching parameter

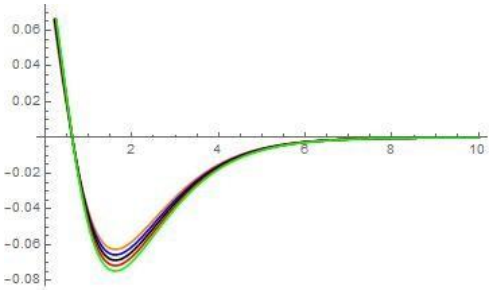

(b) Temperature profile for variants stretching parameter

Figure 3: Solution profile for variants stretching parameter

the effect of the stretching parameter α on both the velocity profile $f(\eta)$ and temperature profile $\theta(\eta)$. It is evident that the velocity profile increases when the stretching parameter α is less than or equal to one, but it decreases when α is greater than one. By contrast, as α increases, the temperature profile declines, and it increases when α decreases. Figures 4. (a-b) illustrates how the hybrid nanofluid volume ratio *phi* affects the skin friction coefficient $Re_x^{1/2}C_f$ and the heat transfer rate $Re_x^{-1/2}Nu_x$. It is clear that when the volume ratio phi_2 is increased while keeping ($phi_1 = 0.02$) constant, the skin friction coefficient increases, leading to a reduction in the heat

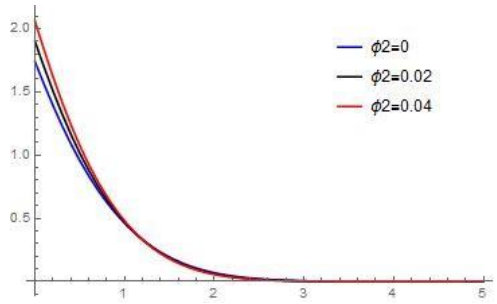

(a) Variation of $Re_x^{1/2}C_f$ for different val-

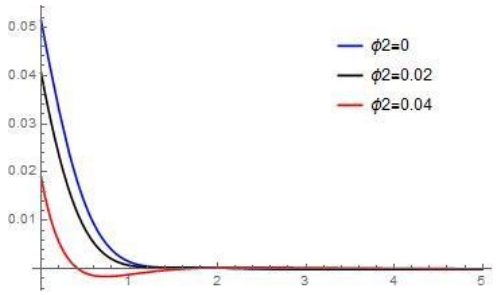

(b) Variation of $Re_x^{-1/2}Nu_x$ for different ues of volume fraction ϕ_2 values of volume fraction ϕ_2

Figure 4: Variation of $Re_x^{1/2}C_f$ and $Re_x^{-1/2}Nu_x$ for different values of volume fraction ϕ_2 transfer rate.

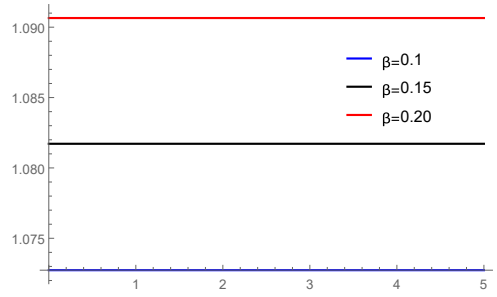

(a) Variation of $Re_x^{1/2}C_f$ with different values of β

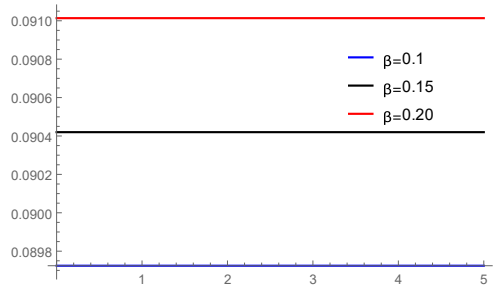

(b) Variation of $Re_x^{-1/2}Nu_x$ with different values of β

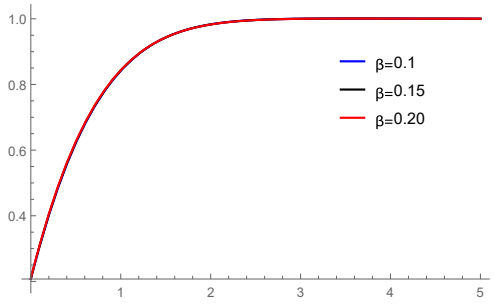

(c) Variation of velocity profile with different values of β

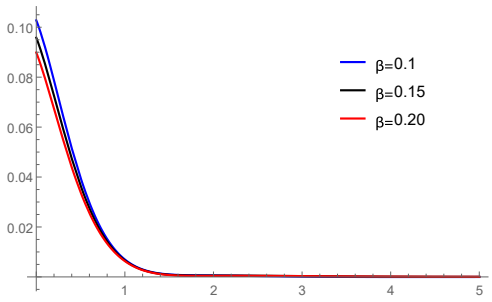

(d) Variation of temperature profile with different values of β

Figure 5: Variation of parameters with different values of β

β leads to a substantial increase in both the skin friction coefficient $Re_x^{1/2}C_f$ and the heat transfer rate $Re_x^{-1/2}Nu_x$, whereas it causes a slight increase in the velocity profile $f'(\eta)$. As illustrated in Figure 5d, the temperature profile $\theta(\eta)$ tended to decrease with an increase in the unsteadiness parameter. Figures 6 shows the velocity distribution $f'(\eta)$ and temperature $\theta(\eta)$ as well as the skin friction coefficient $Re_x^{1/2}C_f$ and heat transfer rate $Re_x^{-1/2}Nu_x$. In Figures 6 (a-b), it is evident that an increase in ϵ results in a decline in both the skin friction coefficient $Re_x^{1/2}C_f$ and heat transfer rate $Re_x^{-1/2}Nu_x$. However, Figures 6 (c-d) show a contrasting trend in the velocity profile $f'(\eta)$ and temperature profile $\theta(\eta)$, respectively. The influence of the variable viscosity parameter Λ on the skin friction coefficient $Re_x^{1/2}C_f$, heat transfer rate $Re_x^{-1/2}Nu_x$, velocity $f'(\eta)$, and temperature $\theta(\eta)$ profiles is illustrated in Figures 7 (a-d). This parameter results in an increase in the values of the skin friction coefficient $Re_x^{1/2}C_f$, heat transfer rate $Re_x^{-1/2}Nu_x$, velocity profile $f'(\eta)$ and temperature profile $\theta(\eta)$. Figure 8 (a-d)

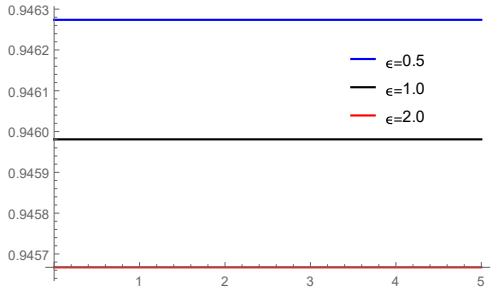

(a) Variation of $Re_x^{1/2}C_f$ with different values of ϵ

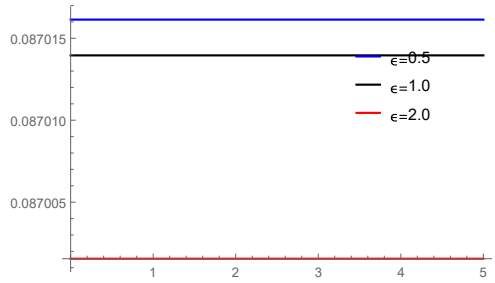

(b) Variation of $Re_x^{-1/2}Nu_x$ with different values of ϵ

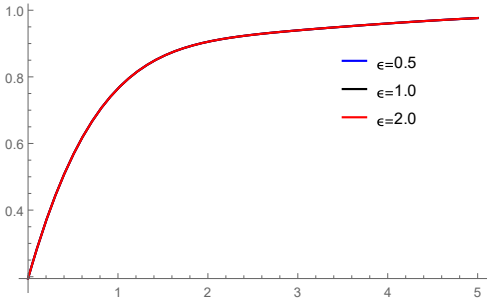

(c) Variation of velocity profile with different values of ϵ

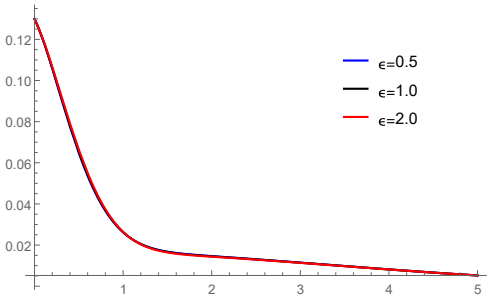

(d) Variation of temperature profile with different values of ϵ

Figure 6: Variation of parameters with different values of variable thermal conductivity coefficient ϵ illustrate the influence of the magnetic parameter M on the skin friction coefficient $Re_x^{1/2}C_f$, heat transfer rate $Re_x^{-1/2}Nu_x$, velocity profile $f'(\eta)$, and temperature profile $\theta(\eta)$. An increase in the magnetic parameter M results in a reduction in the skin friction coefficient $Re_x^{1/2}C_f$, heat transfer rate $Re_x^{-1/2}Nu_x$, and velocity profile $f'(\eta)$, which leads to an increase in the temperature profile $\theta(\eta)$.

Conclusions

In this study, a generalised stagnation-point hybrid nanofluid with varying fluid properties was examined. The nonlinear coupled partial differential equations representing the momentum and energy equations were transformed into a system of coupled nonlinear ordinary differential equations using similarity variables. The transformed system of equations is solved using the Optimal Homotopy Asymptotic Method (OHAM) within the Mathematica package. The following findings are reported: the skin friction coefficient $Re_x^{1/2}C_f$ and heat transfer rate $Re_x^{-1/2}Nu_x$ increase with an increase in the variable viscosity parameter (Λ), unsteadiness parameter (β), and nanoparticle volume fraction (ϕ_2), whereas they decrease with an increase in the variable thermal conductivity parameter (ϵ) and magnetic parameter (M). The velocity profile $f'(\eta)$ increases with an increase in the variable viscosity parameter (Λ), variable thermal conductivity parameter (ϵ), and unsteadiness parameter (β) and decreases with an increase in the volume fraction (ϕ_2) for the stretching parameter (α). The temperature profile $\theta(\eta)$ increases with an increase in the variable viscosity parameter (Λ) and variable thermal conductivity parameter (ϵ) and decreases with an increase in the unsteadiness parameter (β) and volume fraction (ϕ_2) (when the stretching parameter $\alpha > 0$). The impacts of the model parameters were thoroughly analysed. Our findings indicate that the flow and heat transfer rates of the hybrid nanofluid are enhanced by the fluid viscosity, volume fraction of the nanofluid, and variable thermal conductivity. Additionally, the temperature of the hybrid nanofluid was significantly influenced by fluid viscosity and thermal conductivity. However, the nanofluid volume fraction and magnetic.

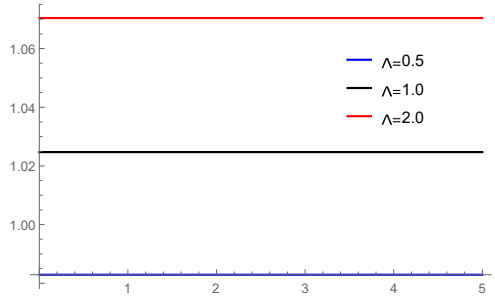

(a) Variation of $Re_x^{1/2}C_f$ with different values of Λ

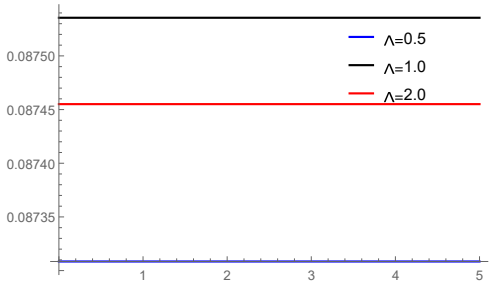

(b) Variation of $Re_x^{-1/2}Nu_x$ with different values of Λ

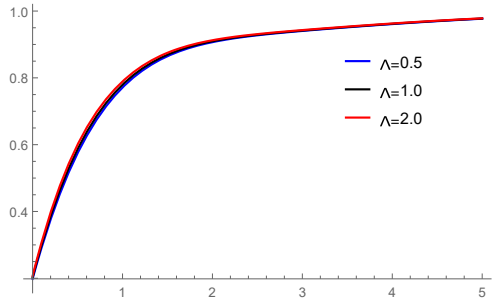

(c) Variation of velocity profile with different values of Λ

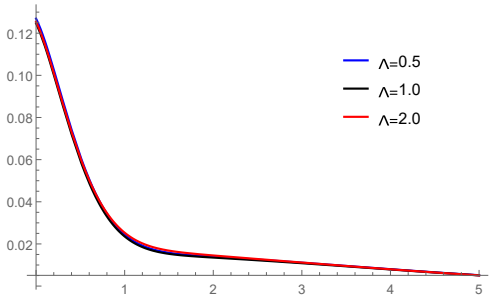

(d) Variation of temperature profile with different values of Λ

Figure 7: Variation of parameters with different values of variable viscosity parameter Λ

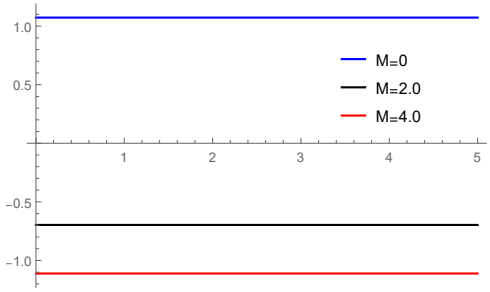

(a) Variation of $Re_x^{1/2}C_f$ with different values of M

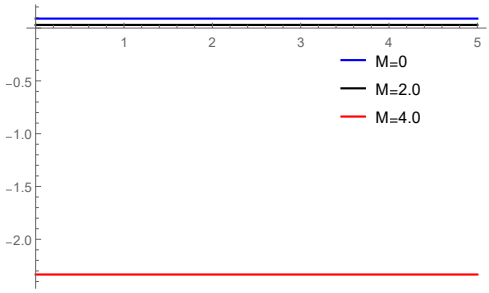

(b) Variation of $Re_x^{-1/2}Nu_x$ with different values of M

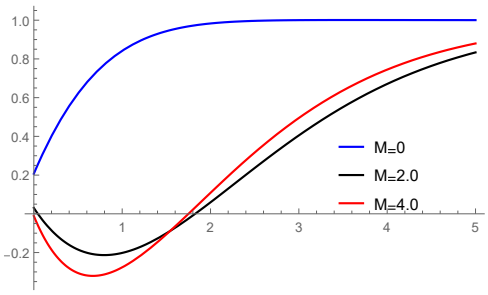

(c) Variation of velocity profile with different values of M

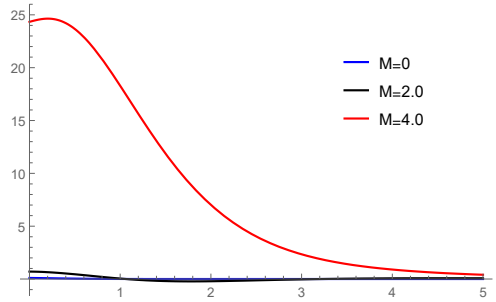

(d) Variation of temperature profile with different values of Λ

Figure 8: Variation of parameters with different values of variable viscosity parameter M parameters inhibited the temperature profile. The values of these parameters can be adjusted to achieve the desired outcomes. The results of this study are applicable to industries such as solar collectors, photovoltaic thermal systems, extrusion processes, polymers, aircraft counter jets, solar extractors, and machined coolants, which can enhance the thermal transmission coefficient of traditional nanoliquids.

Declaration of Competing Interest

The authors declare that they have no known competing financial interests or personal relationships that could have appeared to influence the work reported in this research.

References

1. Ali H Abdelrazek, Omer A Alawi, Salim Newaz Kazi, Nukman Yusoff, Zaira Chowdhury, and Ahmed AD Sarhan. A new approach to evaluate the impact of thermophysical properties of nanofluids on heat transfer and pressure drop. *International Communications in Heat and Mass Transfer*, 95:161–170, 2018.
2. Sarmad Al-Anssari, Ahmed Barifcani, Alireza Keshavarz, and Stefan Iglauer. Impact of nanoparticles on the co2-brine interfacial tension at high pressure and temperature. *Journal of colloid and interface science*, 532:136–142, 2018.
3. Abdullah Al-Yaari, Dennis Ling Chuan Ching, Hamzah Sakidin, Mohana Sundaram Muthuvalu, Mudasar Zafar, Yousif Alyousifi, Anwar Ameen Hezam Saeed, and Muhammad Roil Bilad. Thermophysical properties of nanofluid in two-phase fluid flow through a porous rectangular medium for enhanced oil recovery. *Nanomaterials*, 12(6):1011, 2022.
4. Liaqat Ali, Saeed Islam, Taza Gul, Ali Saleh Alshomrani, Ilyas Khan, and Aurangzeb Khan. Magnetohydrodynamics thin film fluid flow under the effect of thermophoresis and variable fluid properties. *AIChE Journal*, 63(11):5149–5158, 2017.
5. Liaqat Ali, Asifa Tassaddiq, Rohail Ali, Saeed Islam, Taza Gul, Poom Kumam, Safyan Mukhtar, Noor Saeed Khan, and Phatiphat Thounthong. A new analytical approach for the research of thin-film flow of magneto hydrodynamic fluid in the presence of thermal conductivity and variable viscosity. *ZAMM-Journal of Applied Mathematics and Mechanics/Zeitschrift fu¨r Angewandte Mathematik und Mechanik*, 101(2):e201900292, 2021.
6. Emad H Aly and I Pop. Mhd flow and heat transfer near stagnation point over a stretching/shrinking surface with partial slip and viscous dissipation: Hybrid nanofluid versus nanofluid. *Powder Technology*, 367:192–205, 2020.
7. WH Azmi, K Abdul Hamid, Rizalman Mamat, KV Sharma, and MS Mohamad. Effects of working temperature on thermo-physical properties and forced convection heat transfer of tio2 nanofluids in water–ethylene glycol mixture. *Applied Thermal Engineering*, 106:1190– 1199, 2016.
8. Hamza Babar and Hafiz Muhammad Ali. Towards hybrid nanofluids: preparation, thermophysical properties, applications, and challenges. *Journal of Molecular Liquids*, 281:598–633, 2019.
9. Lotfi Ben Said, Lioua Kolsi, Kaouther Ghachem, Mohammed Almeshaal, and Chemseddine Maatki. Advancement of nanofluids in automotive applications during the last few years a comprehensive review. *Journal of Thermal Analysis and Calorimetry*, pages 1–28, 2021.
10. Uddhaba Biswal, Snehashish Chakraverty, Bata Krushna Ojha, and Ahmed Kadhim Hussein. Numerical investigation on nanofluid flow between two inclined stretchable walls by optimal homotopy analysis method. *Journal of Computational Science*, 63:101759, 2022.
11. S US Choi and Jeffrey A Eastman. Enhancing thermal conductivity of fluids with nanoparticles. Technical report, Argonne National Lab. (ANL), Argonne, IL (United States), 1995.
12. Hamed Eshgarf, Rasool Kalbasi, Akbar Maleki, Mostafa Safdari Shadloo, and Arash Karimipour. A review on the properties, preparation, models and stability of hybrid nanofluids to optimize energy consumption. *Journal of Thermal Analysis and Calorimetry*, 144:1959– 1983, 2021.

13. Mehdi Fakour, Davood Domiri Ganji, and Alireza Ahmadi. *Applications of Magnetohydrodynamics for Heat Transfer Enhancement*. Cambridge Scholars Publishing, 2023.
14. Munish Gupta, Vinay Singh, Rajesh Kumar, and Zafar Said. A review on thermophysical properties of nanofluids and heat transfer applications. *Renewable and Sustainable Energy Reviews*, 74:638–670, 2017.
15. Tasawar Hayat, Farwa Haider, Taseer Muhammad, and Ahmed Alsaedi. Darcy–forchheimer three-dimensional flow of carbon nanotubes with nonlinear thermal radiation. *Journal of Thermal Analysis and Calorimetry*, 140:2711–2720, 2020.
16. Guangtao Hu, Xing Ning, Muzamil Hussain, Uzair Sajjad, Muhammad Sultan, Hafiz Muhammad Ali, Tayyab Raza Shah, and Hassaan Ahmad. Potential evaluation of hybrid nanofluids for solar thermal energy harvesting: A review of recent advances. *Sustainable Energy Technologies and Assessments*, 48:101651, 2021.
17. Gabriela Huminic and Angel Huminic. Heat transfer characteristics of a two-phase closed thermosyphons using nanofluids. *Experimental Thermal and Fluid Science*, 35(3):550–557, 2011.
18. Ahmed A Hussien, Wael Al-Kouz, Nadiahnor Md Yusop, Mohd Z Abdullah, and Ayub Ahmed Janvekar. A brief survey of preparation and heat transfer enhancement of hybrid nanofluids. *Journal of Mechanical Engineering/Strojnı˘ski Vestnik*, 65, 2019.
19. F Iriaye, AA Noiki, OO Yusuf, SA Afolalu, and ME Egbe. Overview of nanofluid applications and its sustainability. *Advanced Manufacturing in Biological, Petroleum, and Nanotechnology Processing: Application Tools for Design, Operation, Cost Management, and Environmental Remediation*, pages 45–54, 2022.
20. Furqan Jamil and Hafiz Muhammad Ali. Applications of hybrid nanofluids in different fields. In *Hybrid nanofluids for convection heat transfer*, pages 215–254. Elsevier, 2020.
21. MA Khairul, Elham Doroodchi, Reza Azizian, and Behdad Moghtaderi. Advanced applications of tunable ferrofluids in energy systems and energy harvesters: A critical review. *Energy Conversion and Management*, 149:660–674, 2017.
22. M Riaz Khan, Mingxia Li, Shipeng Mao, Rashid Ali, and Suliman Khan. Comparative study on heat transfer and friction drag in the flow of various hybrid nanofluids effected by aligned magnetic field and nonlinear radiation. *Scientific Reports*, 11(1):3691, 2021.
23. Masood Khan, Muhammad Yasir, Ali Saleh Alshomrani, Sivanandam Sivasankaran, Yaser Rajeh Aladwani, and Awais Ahmed. Variable heat source in stagnation-point unsteady flow of magnetized oldroyd-b fluid with cubic autocatalysis chemical reaction. *Ain Shams Engineering Journal*, 13(3):101610, 2022.
24. Noor Saeed Khan, Saeed Islam, Taza Gul, Ilyas Khan, Waris Khan, and Liaqat Ali. Thin film flow of a second grade fluid in a porous medium past a stretching sheet with heat transfer. *Alexandria Engineering Journal*, 57(2):1019–1031, 2018.
25. Dattatraya P Kshirsagar and MA Venkatesh. A review on hybrid nanofluids for engineering applications. *Materials Today: Proceedings*, 44:744–755, 2021.
26. D Dhinesh Kumar and A Valan Arasu. A comprehensive review of preparation, characterization, properties and stability of hybrid nanofluids. *Renewable and Sustainable Energy Reviews*, 81:1669–1689, 2018.
27. Qingyi Luo, Changhong Wang, and Chili Wu. Study on heat transfer performance of immersion system based on sic/white mineral oil composite nanofluids. *International Journal of Thermal Sciences*, 187:108203, 2023.
28. Younes Menni, Ali J Chamkha, and Houari Ameur. Advances of nanofluids in heat exchangers a review. *Heat Transfer*, 49(8):4321–4349, 2020.
29. John Philip and Porumpathparambil Da Shima. Thermal properties of nanofluids. *Advances in colloid and interface science*, 183:30–45, 2012.
30. Sajjad Porgar, Hakan F Oztop, and Somayeh Salehfekr. A comprehensive review on thermal conductivity and viscosity of nanofluids and their application in heat exchangers. *Journal of Molecular Liquids*, page 122213, 2023.
31. A Renuka Prasad, Sumer Singh, and Harish Nagar. A review on nanofluids: properties and applications. *Int. J. Adv. Res. Innov. Ideas Educ*, 3(3):3185–3209, 2017.
32. Neelu Raina, Preeti Sharma, Parvez Singh Slathia, Deepali Bhagat, and Atin Kumar Pathak. Efficiency enhancement of renewable energy systems using nanotechnology. *Nanomaterials and Environmental Biotechnology*, pages 271–297, 2020.
33. Muhammad Saqib, Ilyas Khan, Sharidan Shafie, and Ahmad Qushairi. Recent advancement in thermophysical properties of nanofluids and hybrid nanofluids: an overview. *City Univ. Int. J. Comput. Anal*, 3(2):16–25, 2019.
34. Yukta Sawant, Kunal Pathare, Rakesh Patel, and Prathamesh Choughule. Nanofluids with recent application & future trends. *International journal of innovations in engineering research and technology*, 8(6):458–468, 2021.
35. Tayyab Raza Shah, Hasan Koten, and Hafiz Muhammad Ali. Performance effecting parameters of hybrid nanofluids. In *Hybrid nanofluids for convection heat transfer*, pages 179–213. Elsevier, 2020.
36. M Sheikholeslami and SA Shehzad. Numerical analysis of fe3o4–h2o nanofluid flow in permeable media under the effect of external magnetic source. *International Journal of Heat and Mass Transfer*, 118:182–192, 2018.
37. Mohsen Sheikholeslami and MK Sadoughi. Simulation of cuo-water nanofluid heat transfer enhancement in presence of melting surface. *International Journal of Heat and Mass Transfer*, 116:909–919, 2018.

38. Nor Azwadi Che Sidik, Muhammad Noor Afiq Witri Mohd Yazid, and Rizalman Mamat. Recent advancement of nanofluids in engine cooling system. *Renewable and Sustainable Energy Reviews*, 75:137–144, 2017.
39. Robert A Taylor, Patrick E Phelan, Todd P Otanicar, Ronald Adrian, and Ravi Prasher. Nanofluid optical property characterization: towards efficient direct absorption solar collectors. *Nanoscale research letters*, 6:1–11, 2011.
40. M. Usman, M. Hamid, T. Zubair, Rizwan Ul Haq, and W. Wang. Cu-al2o3/water hybrid nanofluid through a permeable surface in the presence of nonlinear radiation and variable thermal conductivity via lsm. *International Journal of Heat and Mass Transfer*, 126:1347– 1356, 2018.
41. Muhammad Usman, Muhammad Hamid, Rizwan Ul Haq, and Wei Wang. Heat and fluid flow of water and ethylene-glycol based cu-nanoparticles between two parallel squeezing porous disks: Lsgm approach. *International Journal of Heat and Mass Transfer*, 123:888– 895, 2018.
42. Ravikanth S Vajjha and Debendra K Das. A review and analysis on influence of temperature and concentration of nanofluids on thermophysical properties, heat transfer and pumping power. *International journal of heat and mass transfer*, 55(15-16):4063–4078, 2012.
43. Aleksei A Vozniakovskii, Tatyana S Kol'tsova, Alexander P Voznyakovskii, Alexander L Kumskov, and Sergey V Kidalov. Powder hybrid nanomaterial: Detonation nanodiamonds carbon nanotubes and its stable reversible water nanofluids. *Journal of colloid and interface science*, 565:305–314, 2020.
44. Hassan Waqas, Shan Ali Khan, Metib Alghamdi, and Taseer Muhammad. Numerical investigation for radiative transport in magnetized flow of nanofluids due to moving surface. *Mathematical Problems in Engineering*, 2021:1–10, 2021.
45. Humaira Yasmin, Solomon O Giwa, Saima Noor, and Mohsen Sharifpur. Experimental exploration of hybrid nanofluids as energy-efficient fluids in solar and thermal energy storage applications. *Nanomaterials*, 13(2):278, 2023.
46. Nurul Amira Zainal, Roslinda Nazar, Kohilavani Naganthran, and Ioan Pop. Stability analysis of mhd hybrid nanofluid flow over a stretching/shrinking sheet with quadratic velocity. *Alexandria Engineering Journal*, 60(1):915–926, 2021.
47. Nurul Amira Zainal, Roslinda Nazar, Kohilavani Naganthran, and Ioan Pop. Unsteady stagnation point flow past a permeable stretching/shrinking riga plate in al2o3-cu/h2o hybrid nanofluid with thermal radiation. *International Journal of Numerical Methods for Heat & Fluid Flow*, 32(8):2640–2658, 2022.
48. Zeeshan, N Ameer Ahammad, Nehad Ali Shah, Jae Dong Chung, and Muhammad Shoaib Khan. Computational and stability analysis of mhd time-dependent thermal reaction flow impinging on a vertical porous plate enclosing magnetic prandtl number and thermal radiation effect. *Mathematics*, 11(6):1376, 2023.

CITATION

M. S. Dada, & F. J. Fawehinmi. (2025). A Generalized Hybrid Nanofluid Model Transports with Magnetic, Suction, Velocity Slip, And Varying Viscosity and Thermal Conductivity. In Global Journal of Research in Engineering & Computer Sciences (Vol. 5, Number 3, pp. 112–123).
https://doi.org/10.5281/zenodo.15731771